



Strathprints Institutional Repository

Garcia, David and Trendafilova, Irina (2014) A multivariate data analysis approach towards vibration analysis and vibration-based damage assessment : application for delamination detection in composite materials. Journal of Sound and Vibration, 333 (25). pp. 7036-7050. ISSN 0022-460X , <http://dx.doi.org/10.1016/j.jsv.2014.08.014>

This version is available at <http://strathprints.strath.ac.uk/49373/>

Strathprints is designed to allow users to access the research output of the University of Strathclyde. Unless otherwise explicitly stated on the manuscript, Copyright © and Moral Rights for the papers on this site are retained by the individual authors and/or other copyright owners. Please check the manuscript for details of any other licences that may have been applied. You may not engage in further distribution of the material for any profitmaking activities or any commercial gain. You may freely distribute both the url (<http://strathprints.strath.ac.uk/>) and the content of this paper for research or private study, educational, or not-for-profit purposes without prior permission or charge.

Any correspondence concerning this service should be sent to Strathprints administrator: strathprints@strath.ac.uk

A multivariate data analysis approach towards vibration analysis and vibration-based damage assessment. Application for delamination detection in composite materials

David Garcia^{*1}, Irina Trendafilova²

^{*1}Department of Mechanical and Aerospace engineering
University of Strathclyde, Glasgow, United Kingdom
david.garcia@strath.ac.uk

²Department of Mechanical and Aerospace engineering
University of Strathclyde, Glasgow, United Kingdom
irina.trendafilova@strath.ac.uk

Abstract

This paper introduces a novel methodology for structural vibration analysis and vibration-based monitoring which utilises a special type of Principal Components Analysis (PCA), known as Singular Spectrum Analysis (SSA). In this study the methodology is introduced and demonstrated for the purposes of damage assessment in structures using their free decay response. The method's damage assessment properties are first demonstrated on a numerical example for a two degree-of-freedom (2DOF) spring-mass and damper system with non-linear stiffness. The method is then applied to an experimental case study of a composite laminate beam. The method is based on the decomposition of the frequency domain structural variation response using new variables, the Principal Components (PCs). Only a certain number of the new variables are used to approximate the original vibration signal with very good accuracy. The presented results demonstrate the potential of the method for vibration based signal reconstruction and damage diagnosis. The healthy and the different damaged scenarios are clearly distinguishable in the new space of only two reconstructed components where a strong clustering effect is observed.

Nomenclature

\mathbf{x}	Original data vector in time domain	M	Number of realisations (time series)
\mathbf{X}	Original data matrix in time domain	\mathbf{C}_Z	Covariance matrix of \mathbf{Z}
\mathbf{z}	Original data vector in frequency domain	k	Dimension of the eigen-decomposition
\mathbf{Z}	Original data matrix in frequency domain	ρ_k	Eigen-vectors
$\check{\mathbf{X}}$	Embedded matrix in time domain	λ_k	Eigen-values
$\check{\mathbf{z}}$	Lagged vector in frequency domain	\mathbf{E}_Z	Eigen-vectors in columns matrix
$\check{\mathbf{Z}}$	Embedded matrix in frequency domain	\mathbf{E}'_Z	Eigen-vectors in columns transposed matrix
$\check{\mathbf{Z}}'$	Embedded transposed matrix in frequency domain	$\mathbf{\Lambda}_Z$	Eigen-values in a diagonal matrix
W	Window length	\mathbf{A}	Principal Components matrix
N	Vector length in time domain	\mathbf{R}	Reconstructed Components
N'	Vector length in frequency domain		

1 Introduction

Vibration-based structural health monitoring (VSHM) uses information extracted from the structural vibration response in order to make conclusions about the presence of damage in a structure, its location and its severity [23, 26]. It presents an attractive possibility for structural health monitoring since it is a global non-destructive monitoring method which does not require any *a priori* knowledge about the fault location. It has become increasingly popular from an application and a research view point.

VSHM methods can be divided in two main groups: model based methods and non-model based ones [4]. The model-based methods make use of a model of the structure considered in order to make conclusions for the presence, the location and the extent of the damage present. Most structural dynamic models are linear, while most real structures contain nonlinearities, which include geometric and/or material ones, as well as nonlinearities related to the boundary conditions. For structures with strong nonlinear behaviour, linear models do not give a proper approximations. Accordingly for structures with strong/well expressed nonlinear dynamic behaviour purely data-based modelling, reconstruction and monitoring methods are preferable since they do not assume any model or linearity. Composite materials are one such example. They are known to have well pronounced nonlinear dynamic behaviour while on the other hand monitoring is a must for such materials.

The non model-based dynamic modelling and damage assessment methods make use of the measured signals in order to extract information for the structure itself and for its health. These methods can operate in the time or in the frequency domain and/or they can be based on experimental modal analysis. One of the simplest and most straightforward data-based damage assessment methods utilise the measured natural frequencies of the structure. The methods that use time series analysis and/or nonlinear dynamics methods have been gaining

popularity recently. Such methods use the measured time domain structural vibration signals in order to model and/or analyse its dynamic behaviour and to derive conclusions about its health and integrity. Such methods draw their roots from nonlinear dynamics and they make use of Takens' theorem according to which, any dynamic system can be fully reconstructed in a space made of lagged components of its measured time series. Thus if one is able to measure a time dependent variable from a vibrating structure e.g its displacement or acceleration, the lagged components of this time series can be used to make a new space in which its behaviour can be analysed and ultimately reconstructed.

In practice most purely data-based methodologies make use of data analysis and utilise different statistical methods and characteristics. Principal components analysis (PCA) is one such possibility. In general, PCA is a technique used in data analysis to reduce the dimensionality of the available data. Since vibration signals in the time and/or a frequency domain have quite high dimension, it is obviously appropriate to apply such technique to the measured vibration signals. It also has other properties that are advantageous from view point of SHM. The ability of PCA to distinguish among different categories can be used for the purposes of SHM for distinguishing between e.g. signals measured on damaged and non-damaged structures or signals measured on structures with different damaged extends and/or localizations. PCA is useful for categorical data because it possesses a clustering effect in the sense that it reduces the distance between data vectors from the same category, whilst in the same time, increasing the distance between data vectors from different categories.

This is why a number of studies consider the application of PCA for structural damage assessment purposes.

Some of these papers suggest the selection of certain features from the time or frequency domain of the vibration response signals which can be considered as independent and subject them to PCA [25, 24, 13]. Some authors just use the measured time series responses and subject them to PCA [16, 17, 19, 5]. The point is that PCA is generally developed for multiple and independent variables, while time series elements are usually non-independent [11, 6], in the sense that they are correlated. SSA is a specific application of PCA which is developed for time series. The method suggested here uses SSA, rather than PCA, and in this way it takes care of the inter-correlation between the individual time series elements. Also it should be mentioned that most papers that use PCA apply it in the time domain, while we suggest to apply SSA in the frequency domain, because we think that most of the important information about the system vibration as well as about its health is contained in the frequency domain signal rather than in the time domain one [20]. Furthermore SSA is known to uncover the rotational patterns of certain time series. Thus if one considers a time series from the free response of a structure, it will contain information about the modal frequencies and the mode shapes of the structure. From such a perspective it can be argued that SSA should also contain and uncover the modal contents of a freely vibrating structure from its measured free response [12, 21]. But differently from modal analysis SSA will uncover rotational patterns at any frequency rather than at specific frequencies only. From our view point this is extremely appropriate for nonlinearly vibrating structures which exhibit double or very close modes. For the above reasons we are suggesting the application

of SSA for the purposes of structural health monitoring and the method developed here is primarily targeted for nonlinearly vibrating structures and for structures with nonlinearities.

In this paper the method is demonstrated and applied to a composite laminate beam especially since it is meant for application to structures made of composites. Composite materials are at the forefront of the contemporary research due to their wide range of industrial applications. Structures made of composite materials have increasing importance in different industries such as civil engineering, mechanical and aerospace engineering and energy industry among many others. Composite laminates are made of carbon or glass fibres in their majority, and a matrix commonly of an epoxy resin, which is responsible for the hardening of the material. This makes the laminate unique as a structure. Despite their benefits, composite materials have their disadvantages for instance delamination. Due to their layered nature and the interaction between both materials, fibres and matrix, composite materials are prone to different failure modes, the most common of them being delamination, which can cause irreversible damage. Composite materials with the defect of delamination can lose up to 60% of their stiffness and still remain visibly unchanged.

The method suggested here, applies SSA to the frequency domain acceleration signals. From each discretized frequency domain signal a vector is made from the discrete signal values. Each vector is unfolded into a new W -dimensional space which is made of the lagged frequency domain acceleration signals. In this way each measured frequency domain acceleration vector is substituted by a matrix. We assume that one is in possession of a number of realisations of acceleration vectors and embedding them into a higher dimensional space eventually creates our data matrix. Thus, the data matrix is made of multiple realisations of the frequency domain acceleration vector/signals which are unfolded into a higher dimension. PCA is then applied to this data matrix. Using a certain number of PCs it is possible to reconstruct the original acceleration vectors/signals with very high accuracy. Finally for the purposes of visualization we use two-dimensional projections of our original data into the PC space. In this new 2-dimensional PC space it is possible to distinguish between signals from damaged and non-damaged structures as well as between different damage extents.

The rest of the paper is organized as follows, first the suggested method is introduced. It is then applied to a two-degree of freedom spring-mass system to demonstrate its application and properties. The results are analysed in order to extract information about the system at hand. In section §4 the suggested method is applied and demonstrated for damage assessment in the considered simple structure. §5 is devoted to a real case study of a composite laminate beam. Using its measured vibration response, the application of the suggested method for delamination assessment purposes is demonstrated. The paper concludes with discussion regarding the results obtained for the 2-DoF system and the composite laminate beam.

2 The method suggested

2.1 Singular Spectrum Analysis (SSA)

Principal Component Analysis (PCA) is a method developed for multiple component (vector) variables. Usually, in the case of VSHM, the data vectors comprise components of the measured time series, which can be displacements, velocities or accelerations. In general, PCA assumes that the components of the data vectors are independent. In the case of time series, the values are generally non-independent and thus a variation or extension of PCA, called Singular Spectrum Analysis (SSA), provides a better alternative [11]. SSA is simply PCA applied to lagged versions of a single time series variable.

SSA can be used for different purposes including for smoothing the data, finding a trend and for extraction of periodicities in the form of modulated harmonics [7]. More specifically, the method follows the next steps:

a) Embedding: Let us have a time series converted as a vector, with a length N as $\mathbf{x} = (x_1, x_2, \dots, x_N)$. Given the dimension of window length W where $1 < W \leq \frac{N}{2}$, the W -lagged vectors, placed in columns, define the trajectory matrix $\tilde{\mathbf{X}}$ in a phase space. These vectors are padded with zeros to keep the same vector length. The matrix $\tilde{\mathbf{X}}$ "embeds" the data vector \mathbf{x} into a state space made of the lagged \mathbf{x} vectors. The embedding matrix $\tilde{\mathbf{X}}$ is the representation of the system in a succession of overlapping W -dimension vectors of the time series components.

b) Decomposition: The Empirical Orthogonal Functions (EOFs) are the principal directions of the system. They are calculated by the eigen-decomposition of $\frac{\tilde{\mathbf{X}}'\tilde{\mathbf{X}}}{N}$, which is equivalent to a SVD of $\tilde{\mathbf{X}}$. The eigen-decomposition yields k -eigenvalues and k -eigenvectors which defines the orthonormal basis of the decomposition of $\tilde{\mathbf{X}}$.

c) Reconstruction: The EOFs represent the data as a decomposition of the orthogonal basis functions with a certain percentage of variance of the original signal corresponding to each EOF. The data in $\tilde{\mathbf{X}}$ is projected onto the subspace \mathcal{L}^k built by the EOFs. This projection yields the corresponding Principal Components (PCs) [6].

The Principal Components can be in quadrature, but not in phase between each other. The reconstructed components (RCs) are developed to capture the phase of the time series. The set of EOFs and the corresponding PCs define a reconstruction of the original time series.

A full set of RCs contain all the information contained in the original data since no information is lost in the reconstruction process, and the sum of all RCs gives back the original signal [6].

2.2 Multichannel Singular Spectrum Analysis (MSSA)

MSSA is a natural extension of the SSA for multivariate systems. MSSA applies SSA onto several time series. In this case there is more than one time series as $\mathbf{x}^i = (x_1^i, x_2^i, \dots, x_j^i, \dots, x_N^i)$ where $i = 1, 2, \dots, M$ is the number of time series considered (in this case, the number of realisations) and $j = 1, 2, \dots, N$ the number of components in each series. On the other hand

the number of M -realisations chosen must be $M \leq W$, where W is the window length. Each time series \mathbf{x}^i is gathered into a matrix $\mathbf{X} = (\mathbf{x}^1, \mathbf{x}^2, \dots, \mathbf{x}^M)$ which collects the time series in columns. Once data matrix \mathbf{X} is obtained the procedure detailed in §2.1 is applied. The EOFs obtained by the eigen-decomposition contain information from the whole set of the M -realisations. Similarly to SSA, MSSA can be applied to extract oscillatory behaviour from the multivariate series.

2.3 MSSA in frequency domain

MSSA can be applied in the time or in the frequency domain. MSSA in the frequency domain is applied to the spectrum of the time series. Therefore, PCA is applied to the spectral matrix, which operates in the frequency domain [11]. The procedure consists of transfer from the time domain to the frequency domain [11]. The spectral matrix \mathbf{Z} is then subjected to SVD and the spectral EOFs with its principal modulations are obtained. They are analogous to the principal components scores.

This study considers vibration signals in the frequency domain, and it is believed that their spectra are more informative and provides superior signal/noise separation [15]. It also allows to observe oscillatory patterns behaviour in the space and time [11] and the spectrum itself looks much more ordered and informative for the purposes of selecting features. These are some of the reasons why the authors chose to work in the frequency domain.

3 The damage diagnosis procedure

In this study MSSA is applied for the purposes of damage diagnosis. It is used to extract the information from the structural vibration response and to provide insight into the dynamics of the underlying structure. A damage assessment methodology based on the application of MSSA onto the frequency domain measured vibration signals is suggested here. The following paragraphs present the basic steps of the suggested damage assessment methodology. Figure 1 represents the method in a general block diagram.

3.1 Data collection and transformation

The data collected is made up of an acceleration response signal measured on a vibrating structure. Multiple realisations of the acceleration response series are measured. Each time series \mathbf{x}^i is represented as a vector as shown below:

$$\mathbf{x}^i = (\mathbf{x}_1^i, \mathbf{x}_2^i, \dots, \mathbf{x}_j^i, \dots, \mathbf{x}_N^i)' \quad (1)$$

where $i = 1, 2, \dots, M$ is the number of realisations and $j = 1, 2, \dots, N$ is the number of components in each signal (acceleration vector).

A matrix which collects all the M - realisations of the vectors \mathbf{x}^i is defined as

$$\mathbf{X} = (\mathbf{x}^1, \mathbf{x}^2, \dots, \mathbf{x}^M) \quad (2)$$

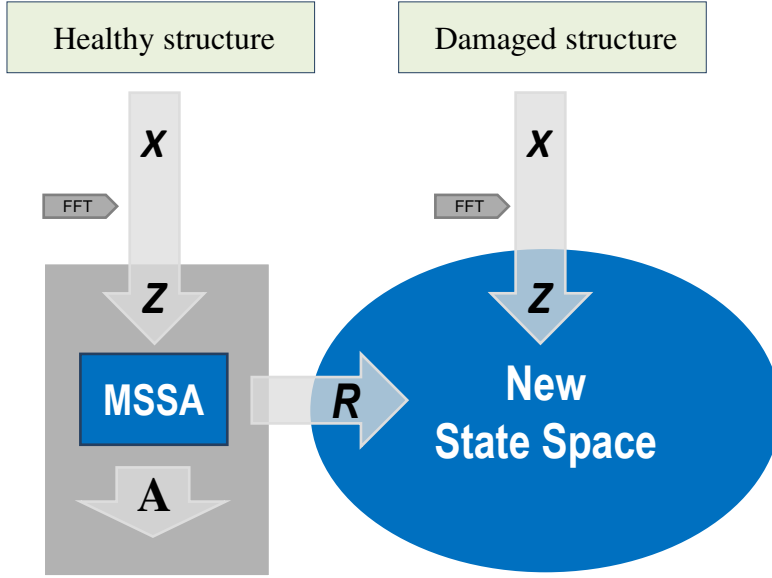


Figure 1: General block diagram of the method

The matrix \mathbf{X} contains the vectors \mathbf{x}^i as columns. Due to the different scales and magnitudes in the measurements, the original data matrix is standardised to ensure consistency in the amplitude values [22].

The time series corresponding to each realisation in the data matrix \mathbf{X} , is transformed into the frequency domain. In this way the spectral data matrix \mathbf{Z} is obtained.

$$\mathbf{Z} = (\mathbf{z}^1, \mathbf{z}^2, \dots, \mathbf{z}^M) \quad (3)$$

Each vector \mathbf{z}^i of the matrix \mathbf{Z} has a length N' where $N' = 1, 2, \dots, \frac{N}{2}$.

$$\mathbf{z}^i = (\mathbf{z}_1^i, \mathbf{z}_2^i, \dots, \mathbf{z}_j^i, \dots, \mathbf{z}_{N'}^i)' \quad (4)$$

3.2 Embedding and Empirical Orthogonal Functions (EOFs)

The next step is to embed the frequency domain signals into a new space. Dynamic systems cannot be fully unfolded in the two dimensional space of their measured signals due to their highly complex behaviour. By creating an embedding space, more dimensions are introduced and thus more features of the original system dynamics are uncovered. According to Takens theorem [2], any dynamic system can be fully unfolded in a new space made of vectors which are lagged versions of the initial time domain signals. This study suggests an embedding of the frequency domain rather than the time domain signals. This is because it is suggested that more information about the dynamic system is contained in a measured frequency domain signal rather than in the time domain one.

A W -dimensional space is created in which the frequency domain vectors are embedded. In this way a vector \mathbf{z}^i is embedded into (and substituted by) an $(N' \times W)$ matrix $\check{\mathbf{Z}}^i$.

$$\check{\mathbf{Z}}^i = \begin{pmatrix} z_1^i & z_2^i & z_3^i & \cdots & z_w^i & \cdots & z_W^i \\ z_2^i & z_3^i & z_4^i & \cdots & z_{w+1}^i & \cdots & z_{W+1}^i \\ z_3^i & z_4^i & z_5^i & \cdots & z_{w+2}^i & \cdots & z_{W+2}^i \\ z_4^i & z_5^i & z_6^i & \cdots & z_{w+3}^i & \cdots & \vdots \\ z_5^i & z_6^i & \vdots & \cdots & \vdots & \cdots & z_{N'}^i \\ z_6^i & \vdots & \vdots & \cdots & z_{N'}^i & \cdots & 0 \\ \vdots & \vdots & z_{N'}^i & \cdots & 0 & \cdots & 0 \\ \vdots & z_{N'}^i & 0 & \cdots & 0 & \cdots & 0 \\ z_{N'}^i & 0 & 0 & \cdots & 0 & \cdots & 0 \end{pmatrix} \quad (5)$$

where $i = 1, 2, \dots, M$ and $w = 1, 2, \dots, W$. All the matrices $\check{\mathbf{Z}}^i$ are collected into a new embedding matrix $\check{\mathbf{Z}}$ with a dimension $N' \times (W \cdot M)$ where N' is the number of components for each vector realisation i , and W is the length of the window applied. It can be observed from Eq.(5) that

$$\check{\mathbf{Z}} = (\check{\mathbf{Z}}^1, \check{\mathbf{Z}}^2, \dots, \check{\mathbf{Z}}^M) \quad (6)$$

At the next step, the covariance matrix of the matrix $\check{\mathbf{Z}}$ is obtained.

$$\mathbf{C}_Z = \frac{\check{\mathbf{Z}}' \check{\mathbf{Z}}}{N'} \quad (7)$$

where \mathbf{C}_Z is the Covariance matrix of $\check{\mathbf{Z}}$ and $\check{\mathbf{Z}}'$ is the transpose of $\check{\mathbf{Z}}$. The eigenvalues λ_k and the eigenvectors ρ_k of \mathbf{C}_Z are obtained according to the following expression.

$$\mathbf{C}_Z \rho_k = \lambda_k \rho_k \quad (8)$$

The eigenvalues λ_k are then ordered in the diagonal matrix $\mathbf{\Lambda}_Z$ in decreasing order and the matrix \mathbf{E}_Z contains their corresponding eigenvectors ρ_k written as columns.

$$\mathbf{E}_Z' \mathbf{C}_Z \mathbf{E}_Z = \mathbf{\Lambda}_Z \quad (9)$$

The eigenvalues define the partial variance of each eigenvectors, therefore the total sum of all of these variances gives the total variance of $\check{\mathbf{Z}}$.

3.3 Decomposition and Reconstruction

The EOFs represent the original data as a decomposition in an orthonormal basis with a certain percentage of the variance of the frequency domain signal corresponding to each EOF. Projecting the measured data $\check{\mathbf{Z}}$ onto the EOFs matrix \mathbf{E}_Z yields the corresponding Principal Components matrix \mathbf{A} [6].

$$\mathbf{A} = \check{\mathbf{Z}}\mathbf{E}_Z \quad (10)$$

It is now required to reconstruct the original signal data in terms of the new PCs. For the purpose a matrix which projects the PCs back into the new subspace is created. The Reconstructed Components (RCs) are obtained according to the Eq. (11). For a given set of indices \mathcal{K} corresponding to the set of Principal Components, the RCs are obtained by projecting the corresponding PCs onto the EOFs.

$$R_{m,n}^k = \frac{1}{W} \sum_{w=1}^W A_{n-w}^k E_{m,w}^k \quad (11)$$

where k -eigenvectors give the k^{th} RC at n -frequency between $n = 1 \dots N'$ for each m -realisation ($m = 1 \dots M$) which was embedded in a w -lagged vectors with the maximum W -length.

3.4 Projection and visualisation. Clustering effect

The decomposition of the oscillatory system by a certain number of components generates a new subspace \mathcal{L}^k which is with a dimension k , where k is the number of reconstructed components. The decomposition in terms of the principal components reconstructs the original data into a new orthogonal subspace. The new subspace allows us to reconstruct and represent each vibratory signal by using an inner-product, into a single point. The decomposition of the vibratory signals into a new space, which can contain different number of components k , is given by the projection of this point onto the axes of the subspace \mathcal{L}^k , as it is illustrated in Figure 2. Suppose now that we are dealing with signals from several categories, which correspond to different damage states, including the healthy (non-damaged) state. Each of these categories will generate an original data matrix \mathbf{Z}_p . In order to visualize the results, it is considered only 2-dimensional space. This original data matrix $\vec{\mathbf{Z}}_p$ is now projected onto the unit basis made of the EOFs, $\hat{\mathbf{e}}_1$ and $\hat{\mathbf{e}}_2$, generating the reconstructed components $\vec{\mathbf{r}}_1$ and $\vec{\mathbf{r}}_2$. The inner-product (T_1, T_2) between the original data $\vec{\mathbf{Z}}$ and the reconstructed components $\vec{\mathbf{r}}_1$ and $\vec{\mathbf{r}}_2$ generates the new set of reconstructed coordinates according to Eq. (12).

$$\mathbf{T} = \langle \mathbf{Z}_p, \mathbf{R} \rangle = \sum_{p=1}^P \mathbf{Z}'_p \mathbf{R} \quad (12)$$

where \mathbf{Z}'_p is the original frequency signal matrix of each p -categories and the matrix \mathbf{R} is made of the reconstructed components, which correspond to the healthy structure.

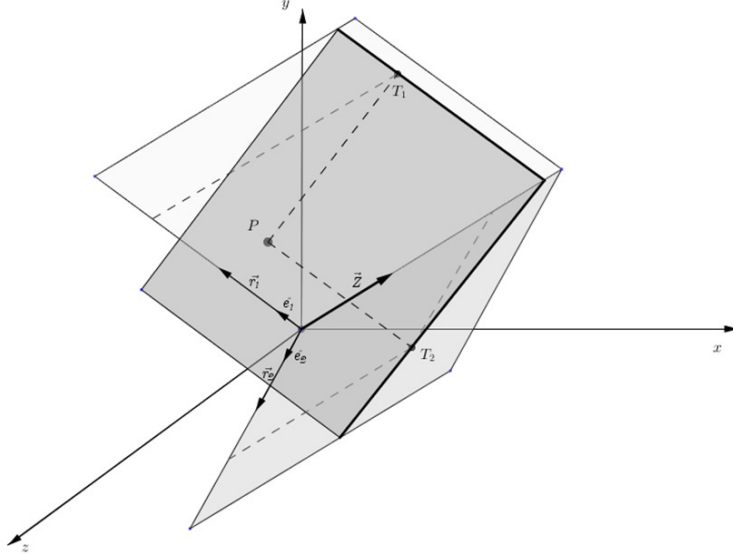


Figure 2: Inner product between RC and original response.

4 Simulated example: 2-DOF nonlinear spring-mass-damper system

4.1 The system

A two degree-of-freedom (DoF) spring-mass and damper system with non-linear stiffness described by a second order ordinary differential equation is considered in order to demonstrate the damage detection procedure described in §3. The system is illustrated in Figure 3 below and is described by Eq. (13).

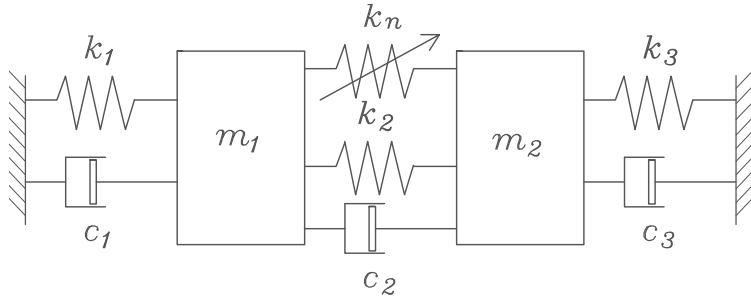


Figure 3: 2-DOF spring-mass damper with non-linear stiffness system

$$[\mathbf{M}]\ddot{\mathbf{x}} + [\mathbf{C}]\dot{\mathbf{x}} + [\mathbf{K}]\mathbf{x} + \mathbf{f}(\dot{\mathbf{x}}, \mathbf{x}) = 0 \quad (13)$$

where $[\mathbf{M}]$, $[\mathbf{C}]$, $[\mathbf{K}]$ are constant coefficients mass, damping and stiffness matrices respectively defined by the Eq. (14). The function $\mathbf{f}(\dot{\mathbf{x}}, \mathbf{x})$ provides a quadratic coupling between

two masses and it is defined by Eq. (15).

$$[\mathbf{M}] = \begin{pmatrix} m_1 & 0 \\ 0 & m_2 \end{pmatrix} \quad [\mathbf{C}] = \begin{pmatrix} c_1 + c_2 & -c_2 \\ -c_2 & c_2 + c_3 \end{pmatrix} \quad [\mathbf{K}] = \begin{pmatrix} k_1 + k_2 & -k_2 \\ -k_2 & k_2 + k_3 \end{pmatrix} \quad (14)$$

$$\mathbf{f}(\dot{\mathbf{x}}, \mathbf{x}) = \begin{Bmatrix} -k_n(x_2 + x_1)^2 \\ k_n(x_2 + x_1)^2 \end{Bmatrix} \quad (15)$$

The following values were considered as initial conditions $x_0^{(1)} = 0m$, $\dot{x}_0^{(1)} = 0m/s$, $x_0^{(2)} = 0m$, $\dot{x}_0^{(2)} = 1m/s$. The values of the stiffness in the system are $k_1 = k_2 = k_3 = 2000N/m$, the damping coefficients are $c_1 = c_2 = c_3 = 6Ns/m$, the masses of the system are $m_1 = m_2 = 5kg$ and the value of the constant coefficient of the quadratic stiffness is $k_n = 10000N/m^2$. The selection of these values is to define a set of baseline conditions which will be altered in order to simulate damaged in the system[18]. The acceleration was obtained from the free-decay response of the system by the numerical integration of the Eq. (13). The acceleration of the m_1 was measured each instant of time for 2.56s long and sampled at 400Hz.

4.2 Damage assessment

The system with the parameters defined as initial conditions presented in §4.1 was considered as a healthy system. Damage was introduced in the system by a certain percentage of stiffness reduction. The stiffnesses of springs k_1 , k_2 and k_n were reduced by 10%, 20% and 30% subsequently.

4.2.1 Natural frequencies and damage assessment

The changes in the natural frequencies are studied with the above stiffness reductions in order to see whether they can provide useful information for the presence of damage/stiffness reduction. It should be mentioned that the effects of delamination/damage on the natural frequencies is usually quite small and this is why in most cases they are not good as damage indicators. The situation is very much the same for the case of this simulated example (see §4.2). The two natural frequencies do not seem to change sufficiently in order to be used as indicators for damage/stiffness reductions.

Figure 4 gives the changes in per cent of the two natural frequencies f_1 and f_2 with the different stiffness changes. It can be seen from Figure 4(a) that the first natural frequency is associated with the reduction in k_1 while the second natural frequency is related to the changes of k_2 (see Figure 4(b)). The first natural frequency f_1 changes for the 20% k_1 reduction but it is not affected by the 10% reduction. Thus only big changes can be detected on the basis of the changes of this frequency. The second natural frequency changes with the reduction of k_2 and it experiences a 6% reduction with the 10% reduction of k_2 , which grows to 12% and 18% for the 20% and the 30% changes of k_2 , respectively. Thus the second natural frequency might be a good indicator for damages related to k_2 , although the 6% change for the 10% stiffness reduction is rather small. But neither f_1 nor f_2 seem to be

related to the changes in the nonlinear stiffness k_n . Thus k_n reductions cannot be detected on the basis of the changes of the natural frequencies. Therefore, accordingly this example demonstrates and stresses on the need for an alternative damage assessment methodology especially for the case of nonlinear damage.

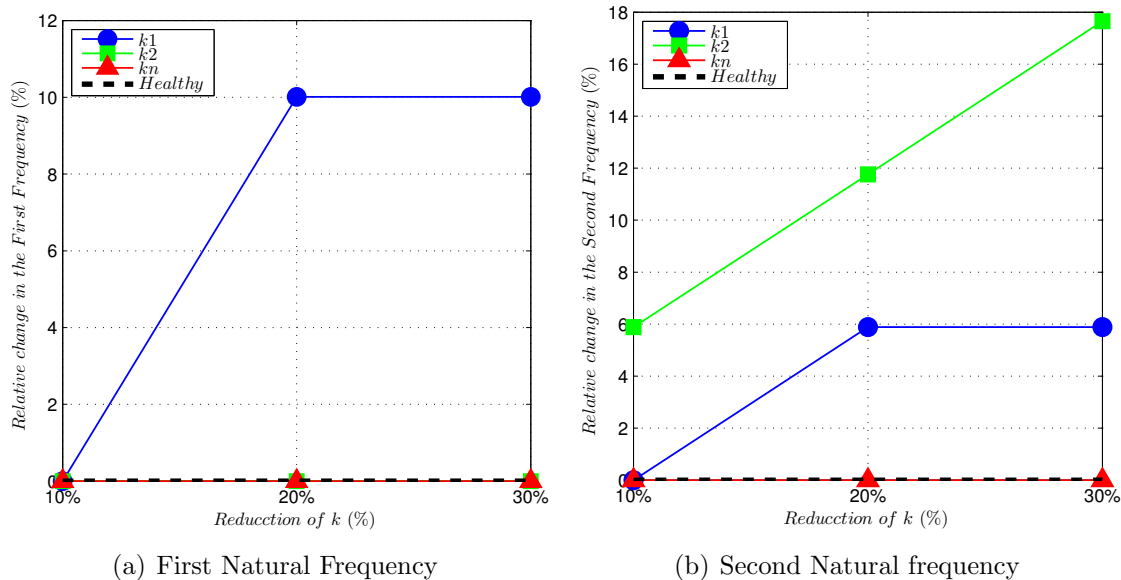
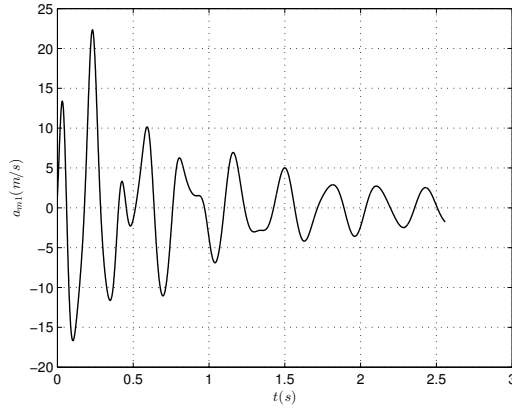


Figure 4: 2 DoF system natural frequencies with stiffness reduction

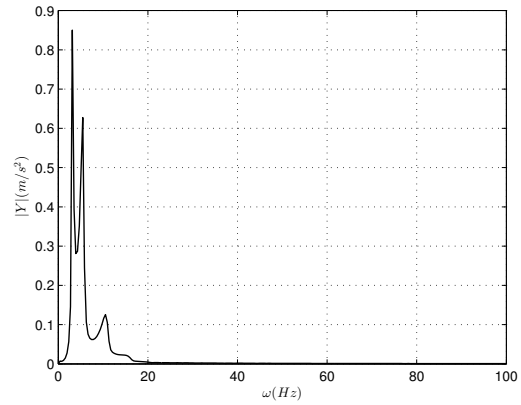
4.2.2 Application of the damage assessment procedure

In this paragraph we detail the application of the damage assessment procedure described in §3 to the case of the 2DoF system considered here. The method presented in §3 was applied on the free-decay acceleration signals obtained. First, the acceleration signals for m_1 were obtained and transformed into the frequency domain. White noise was added to the responses by using the command AWGN in the commercial software Matlab. This command adds White Gaussian Noise by the scalar SNR which specifies the signal-to-noise ratio e.g. in dB. In this case, the additive noise level was set to 20dB. Ten random signals were generated for each scenario, *vz* the healthy system and nine damage scenarios generated by the stiffness reductions scenarios. Figure 5 presents the acceleration signals corresponding to the mass m_1 in the time domain (Figure 5(a)) and in the frequency domain (Figure 5(b)) without noise and Figure 5(c) and Figure 5(d) give an example of the acceleration signals with noise.

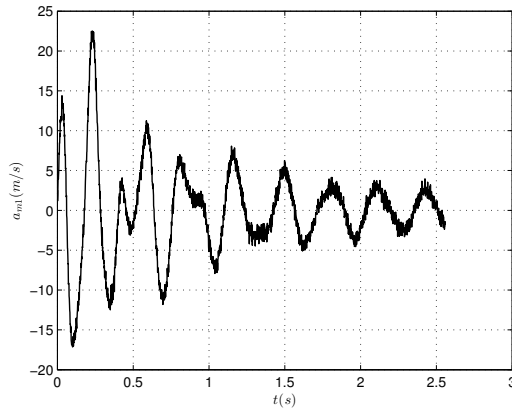
In the case without noise, only one signal from each scenario was used to calculate \mathbf{Z} which corresponds to a single vector with the dimension of $N' = \frac{N}{2} = 1024$ and $M = 1$ realisations. Therefore, the method applied is SSA as defined in §2. However when white noise was added to the responses, the method applied was MSSA defined in §3 because in this case multiple realisations are created. In this case, the matrix \mathbf{Z} was calculated for $N' = 1024$ and $M = 7$. This was applied for each beam scenario.



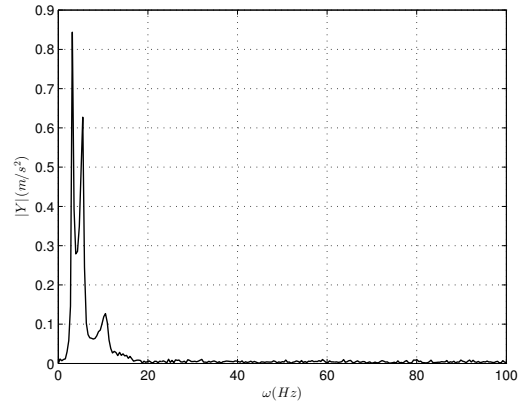
(a) Time domain response without noise



(b) Frequency domain response without noise



(c) Time domain response with 20dB white noise



(d) Frequency domain response with 20dB white noise

Figure 5: 2 DoF system vibration response of the acceleration of m_1 with and without noise for the Healthy case

The window length has a particular significance on the singular spectrum analysis and eventually on the form of the reconstructed signal [3]. The selection of the proper window length depends on the problem at hand and on the preliminary information about the time series [8]. The main principle for selecting a proper window length is to find the value which produces separable and independent principal components. This is important for the accurate reconstruction of the signal. A general aspect in the selection of W is that longer window length will provide more detailed decomposition. According to this statement, the best detailed decomposition should be obtained for $N/2$. Nonetheless a large window length will require more components but it can in the same time introduce more noise in the reconstruction [1]. In this particular case, we tested different window lengths starting from large values of W until the proper effect was achieved. The selection of $W = 7$ is due to its capability to produce a distinguishable clustering effect among the different delamination

scenarios as will be shown below. It should be mentioned that the selection of W depends on the case to study and this value will be different depending on the system considered.

First following the procedure detailed in §3.4 a new subspace is created where the data is more observable and easy to analyse. The procedure is applied with and without noise added to simulated data. The first two reconstructed components for the four categories considered are presented in Figures 6, 7 and 8 for each stiffness reduction, respectively. The dimension of two RCs was chosen for visualization purposes only. The clustering effect is obvious for all the stiffness reduction cases. The ability of developed methodology to detect changes in a vibratory system is successfully demonstrated. From the results, it can be seen that the method is sensitive to the different stiffness changes and hence to the damage location. The use of more RCs will increase the precision in the reconstruction and is thus expected to enhance/improve the recognition effect (the separability of the categories considered). Figures 6(a), 7(a) and 8(a) present the first two RCs without any noise. It can be perceived that RCs corresponding to the different damage scenarios are well separated from each other and thus each of the damage scenarios can be identified clearly.

For the case when white noise is added the first two RCs for each damage scenario are presented in Figures 6(b), 7(b) and 8(b). With noise added the clustering effect between the different categories can be still observed for all damage scenarios. The different damage/stiffness reduction categories related to the different damage sizes, *vz* 10%, 20% and 30% are well separated for the cases of k_1 and k_2 reductions. The situation for k_n reductions is a somewhat worse in terms of separation among the different stiffness reductions categories. It can be seen from Figure 8(b) that the variance within the categories is considerable, which obscures their separation. But still the clustering effect is present for the case of different changes in the non-linear stiffness k_n , and the first two RCs only provide a relatively good separation between the cases of 10%, 20% and 30% k_n reductions.

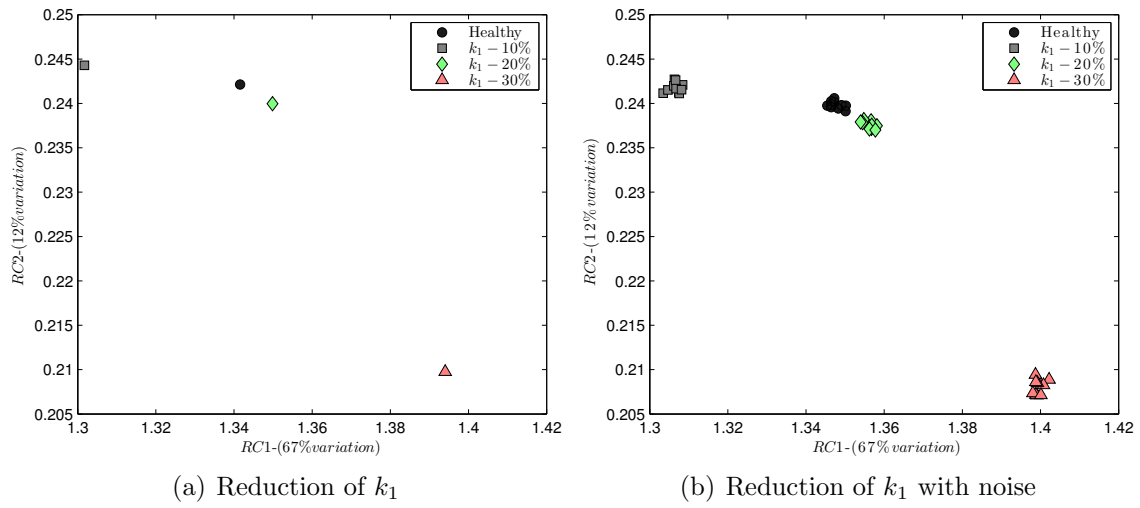


Figure 6: The first two RCs with reduction of k_1

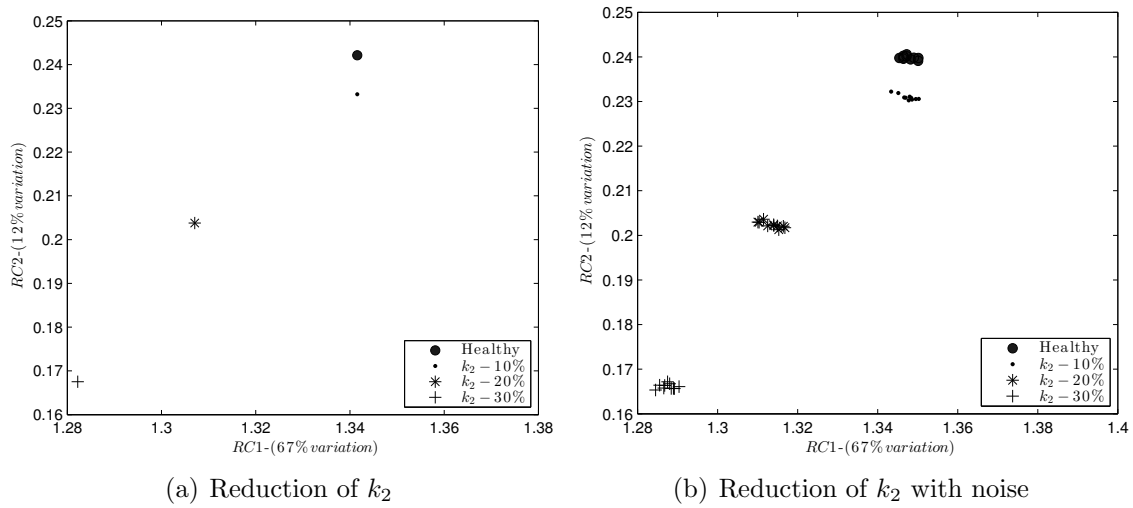


Figure 7: The first two RCs with reduction of k_2

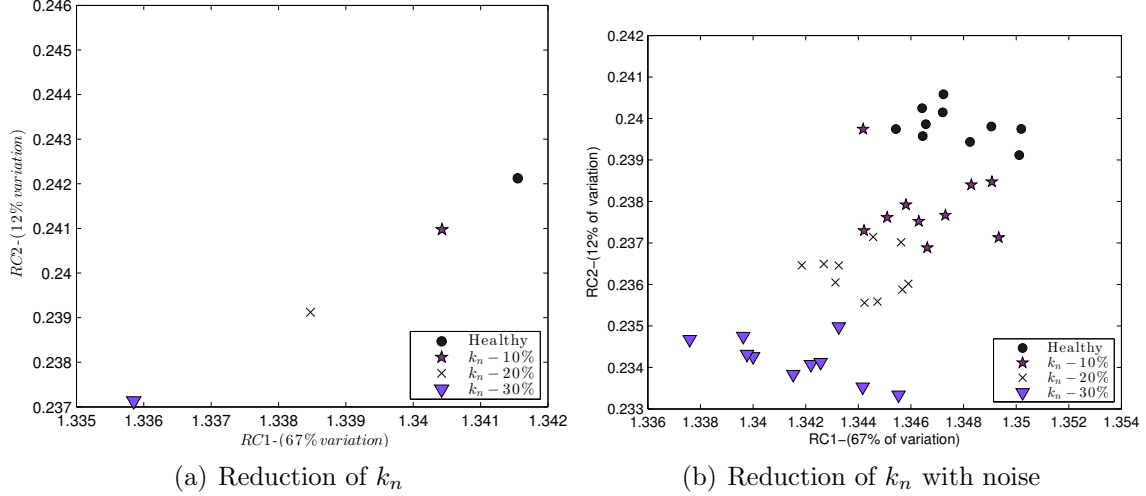


Figure 8: The first two RCs with reduction of k_n

5 Application for a composite laminate beam

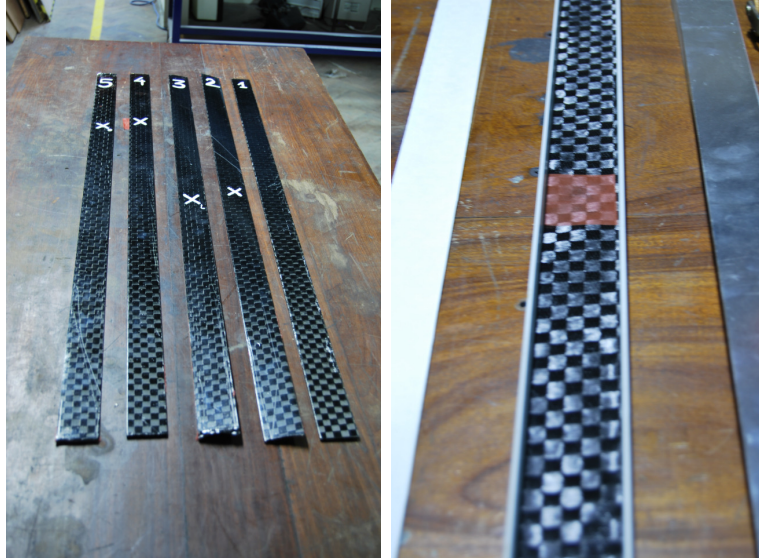
5.1 The structure and the experiment

Five composite laminate beams were manufactured using 10-layered carbon woven laminate multipreg *E722* resin. The dimension of the beams is $980 \times 42 \times 2.5 \text{ mm}$. Each of the beams represents a damage scenario including the one without delamination as detailed in Table 1. The five different scenarios are detailed below and they are shown in Figure 9(a). A small piece of Teflon was introduced to simulate delamination as is shown in Figure 9(b). The non-adherent property of this material disbonds the layers.

Beam	Delamination	Position lengthwise	Position depthwise	Delamination length
<i>B1</i>	<i>Non – delaminated</i>	<i>Non – delaminated</i>	<i>Non – delaminated</i>	<i>Non – delaminated</i>
<i>B2</i>	<i>Middle</i>	<i>5th – 6th layer</i>	<i>50 mm</i>	
<i>B3</i>	<i>Middle</i>	<i>220 mm from edge</i>	<i>5th – 6th layer</i>	<i>80 mm</i>
<i>B3</i>	<i>220 mm from edge</i>	<i>5th – 6th layer</i>	<i>50 mm</i>	
<i>B5</i>	<i>220 mm from edge</i>	<i>2th – 3th layer</i>	<i>50 mm</i>	

Table 1: Composite laminate beams. Delamination scenarios

The beams were fully-fixed at both ends with a free length of 900 mm between the supports. The acceleration of free-decay responses of the specimens was recorded. In Figure 10, a detailed sketch of the experimental set-up is presented.



(a) Five beams scenarios (b) Delamination introduction

Figure 9: Five beams scenarios and delamination introduction

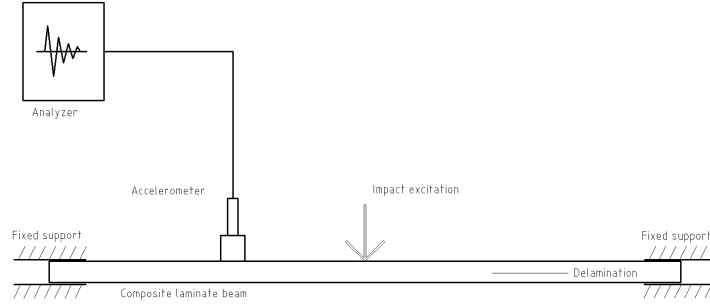


Figure 10: Experiment set-up.

5.2 Data collection and reconstruction

Seven free-decay responses induced by hammering, with a soft hammer, were recorded on each structure. The acceleration signals were fixed at $1.6s$ length and sampled at $640Hz$. Thus, for each damage scenario (for each composite laminate beam) we are in possession of seven data realisations for each acceleration signals ($M = 7$). They are again gathered in five matrices $\mathbf{X}_p = (\mathbf{x}^1, \mathbf{x}^2, \dots, \mathbf{x}^M)$ where $p = 1, 2, \dots, P$ and $P = 5$ is the number of damage scenarios.

The matrix \mathbf{X}_1 corresponds to the healthy structure from the data recorded from beam B1. Based on the healthy structure, which is the baseline condition of the system, MSSA was applied as described in §3.

The time domain responses were first transformed into the frequency domain. Figure 11(a) and Figure 11(b) represent the time and frequency domain responses for one realisation

of the healthy beam.

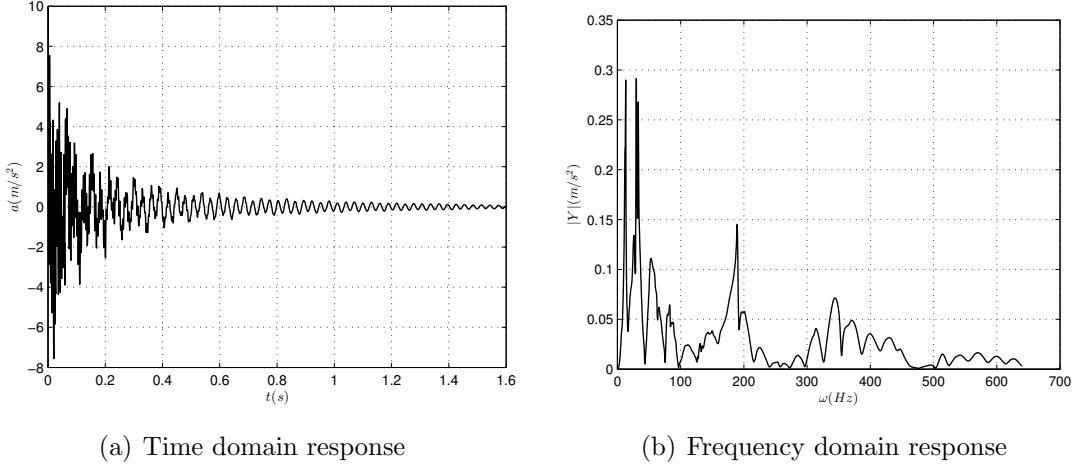


Figure 11: Healthy structure vibration response Beam 1 realization 1 (B1-1)

The data matrix \mathbf{Z} is then constructed using the M –realisations of the N' –dimensional frequency domain values (in our case $N' = 1024$). The procedure explained in §3, was applied to the frequency domain data matrix \mathbf{Z} . A window size $W = 7$ was chosen for the purposes of this investigation. The reasoning for this was explained in §4.2.

The Principal Components (PCs) were obtained by projection of the original data onto the EOFs. Nearly 100% (93%) of the whole variance is contained in the first nine EOFs. The first two EOFs are responsible for 88% of the variance where the 83% comes from the first one and 5% from the second one. After the first four EOFs, the low percentage of variance remains constant for the subsequent EOFs, as is shown in Figure 12. In Figure 12, only fifteen components are shown since after the ninth component, the percentage of variance for the rest of the components remains very small. The original frequency domain series are eventually reconstructed using the first four Reconstructed Components (RCs).

5.3 Results

The results from the reconstruction using the first four RCs is represented in Figure 13. It can be observed from Figure 13 that the reconstructed signal follows the original frequency domain series more closely, as compared the one reconstructed by using two RCs.

The decomposition in PCs of the original frequency series reduces the distance between the new coordinates for objects from the same category whilst at the same time it increases the distance between objects from different categories. This effect can be seen in Figure 14, which represents the first two RCs of the original signals for the different damage scenarios. A rather strong clustering effect can be observed in Figure 14. The results in Figure 14 show that the method is able to detect the presence of delamination in this experimental case of study. The clusters formed by the RCs corresponding to the different damage scenarios

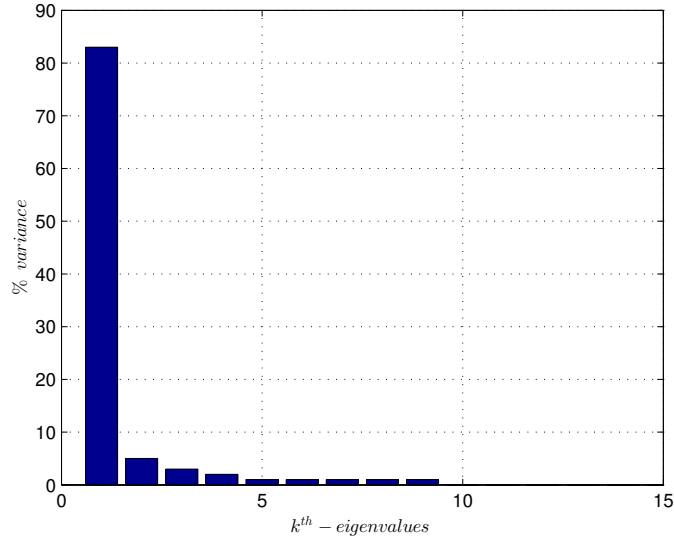


Figure 12: Scree diagram

can be very well distinguished. This means that the methodology is not only able to detect delamination. It is also able to distinguish among the different delamination scenarios which involve different delamination sizes and locations. These results give an additional potential for further development of the methodology towards more precise damage localization and severity evaluation, which will be a goal in our future studies.

6 Discussions

It should be mentioned here that the main aim of this study is to introduce a methodology for damage/delamination detection and assessment and to establish it. This paper attempts crude localization and size estimation in the sense of categorization. Different categories related to different locations and sizes were defined and we were able to prove that the suggested methodology is able to distinguish among them. But currently on the basis of the obtained results we are unable to find any trends or patterns in the PCs with the location and/or the size of the delamination. Thus, at this current stage according to our results, we can only claim that the methodology is able to distinguish among different categories, any other claims will be unsubstantiated. In the following two paragraphs we discuss the results obtained for the 2-DoF system and the experimental case study.

6.1 2DOF system

The first thing to mention is that the suggested method is undoubtedly able to detect the presence of damage/stiffness reduction for all the three cases investigated. For the cases of

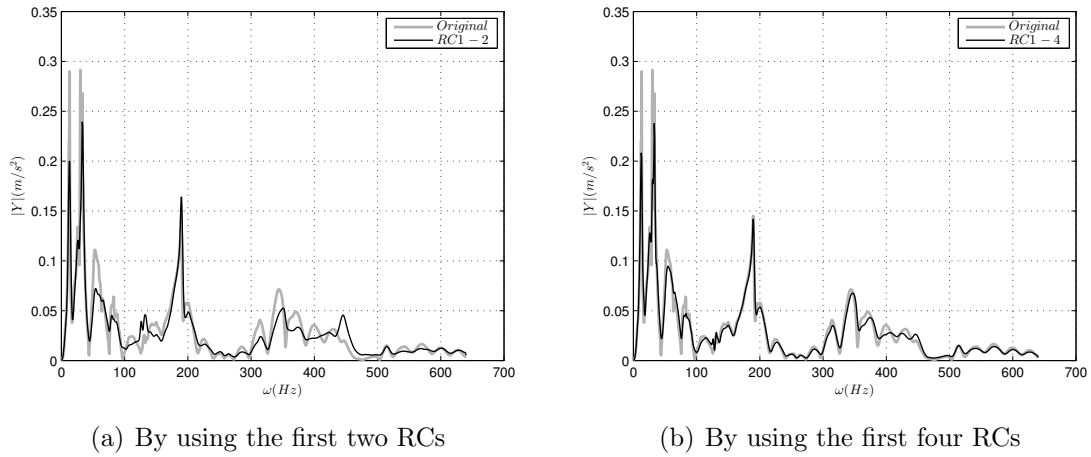


Figure 13: Reconstruction of the original signal

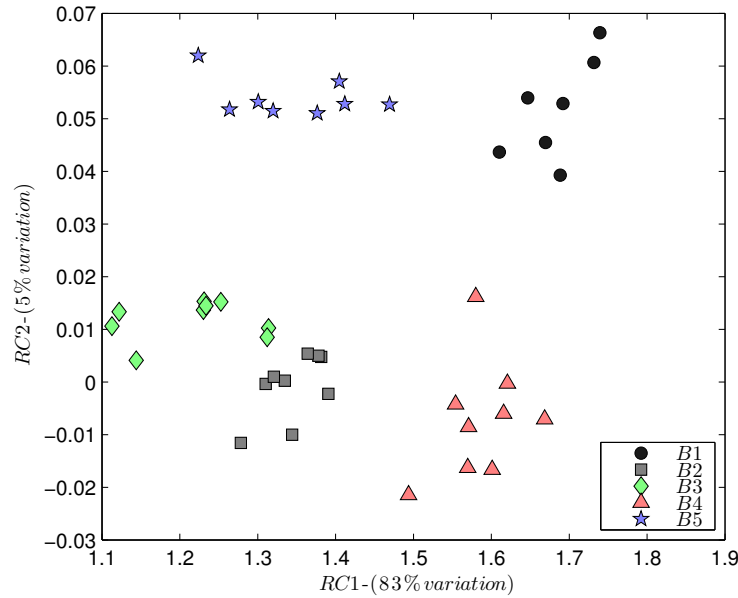


Figure 14: The first two RCs for the case of the experimental case study

k_1 and k_2 reductions the pattern vectors made of the first two reconstructed components are quite far away from the healthy ones. The detection is a bit more biased for the case of k_n reduction, and there are only a couple of pattern vectors that are in the cluster made of the healthy pattern vectors.

Furthermore according to our results for the simulated 2-DoF system the method is able to distinguish among the different categories related to the size of all stiffness reductions, in k_1, k_2 and k_3 . Looking at the results for k_1 one can conclude that the distance between the healthy and the different damage/stiffness reduction categories does not increase with

the increase of damage. But on the other hand $RC2$ seems to decrease with damage so it might be used as a feature. According to the other graphs related to k_2 and k_3 reductions, the distance between the healthy vectors and the damaged ones does increase with the size of damage/stiffness reduction. But the establishment of a pattern or trend in any of the RCs is still a matter of further investigation and we need more results in order to be able to answer questions related to the capabilities of the methodology related to size and location estimation.

6.2 The composite beam application

The next application is on a real example of a composite beam. In this case again we can say that detection can be achieved even in the case of the smaller delamination, which is 50mm (5% of the total length of the beam). Regarding the experimental case study again at this stage we only attempted crude (categorical) localization and size estimation in terms of categorization. In this case different lengths and different locations of the delamination are introduced. Again with the use of only the first two reconstructed components, the methods clustering abilities are able to distinguish between the different categories, as shown in Figure 14. The clusters are quite well defined in terms of location as well as in terms of delamination extent. The two sets that correspond to different extent of the delamination are fairly close to each other. Accordingly for this case study we were able to prove that the method can provide this type of categorization and in such a sense it can provide crude localization and size estimation. Our results show that the categories defined are well distinguishable and one can draw boundaries among them to help the recognition process. In this case again, similarly to the simulated example, it is still rather early to talk about size estimation and localization because it is difficult to establish a trend or pattern with the change of the location and/or the size of delamination. What it can claim at the moment is categorical estimation and localization. A further systematic investigation with different sizes and locations of the delamination is needed in order to be able to say if the method is able to provide more precise localization and size estimation.

A further development in terms of damage and delamination diagnosis will be to increase the number of reconstructed components used to model the vibratory behaviour, which are actually used as features in the diagnosis process. This obviously improves the reconstruction of the measured signal and will increase the diagnosis capabilities of the suggested method as shown in Figure 13. It should be noted that the distances between the different categories/clusters in Figure 14 are rather small. Thus an enhancement procedure is desirable which will increase the distances between the different categories. Work is currently being undertaken to address this issue.

In this study just the two dimensional space of the first two RCs was used mainly for visualisation purposes, but a pattern recognition approach can be developed in higher dimension space using more RCs, which will increase the capabilities of the suggested method.

7 Conclusions

In this paper a methodology is suggested, which utilizes MSSA for the purposes of vibration analysis and damage assessment in structures using their free decay response. This study uses the methodology for the purposes of vibration-based damage assessment and it demonstrates its application for two case studies. The main aim of this study is to introduce and establish the method and we do this using two applications: for a simulated 2 DoF system and for an experimental case study of a composite beam. At this stage we have attempted damage and delamination detection and we have studied the changes of the first two PCs with different sizes and extents of the damage. Our results show that the first two PCs can be used for damage/delamination detection and furthermore they can be used for categorical damage estimation and localization. Thus at this stage we only claim crude capabilities of the method for localization and size estimation in terms of rather large categories defined. More precise damage estimation and localization are objects of further studies in order to establish different capabilities of the introduced methodology.

The authors would like to stress that (to their knowledge) this is a pioneering study which introduces the application of singular spectrum analysis and multichannel spectrum analysis in the frequency domain for damage assessment in vibrating structures. SSA and MSSA have been applied mainly in climatology, economics and medicine among many others [9, 10, 14]. It is the opinion of the authors that the suggested methodology has a much greater potential extending far beyond damage assessment and this study only provides a demonstration for one potential application. It can be used for modelling purposes, which appears to be one of the most important potential applications since it can allow modelling from data for nonlinearly vibrating structures. Other possible applications which are relevant and beneficial for vibrating structures include trend estimation and detection and estimation of periodicities and nonlinear rotational patterns. These are again important for vibration analysis especially for nonlinearly vibrating structures, since these applications can be used in place of modal analysis.

References

References

- [1] FJ Alonso, JM Del Castillo, and P Pintado. Application of singular spectrum analysis to the smoothing of raw kinematic signals. *Journal of biomechanics*, 38(5):1085–1092, 2005.
- [2] Daniela Baratta, Giovambattista Cicioni, Francesco Masulli, and Léonard Studer. Application of an ensemble technique based on singular spectrum analysis to daily rainfall forecasting. *Neural Networks*, 16(3):375–387, 2003.
- [3] DS Broomhead and Gregory P King. Extracting qualitative dynamics from experimental data. *Physica D: Nonlinear Phenomena*, 20(2):217–236, 1986.

- [4] E.Peter Carden and Paul Fanning. Vibration based condition monitoring: A review. *Structural Health Monitoring*, 3(4):355–377, 2004.
- [5] Mario Anderson de Oliveira, Jozue Vieira Filho, Vicente Lopes Jr, and Daniel J Inman. Damage detection based on electromechanical impedance principle and principal components. In *Topics in Modal Analysis, Volume 7*, pages 307–315. Springer, 2014.
- [6] Michael Ghil, MR Allen, MD Dettinger, K Ide, D Kondrashov, ME Mann, Andrew W Robertson, A Saunders, Y Tian, F Varadi, et al. Advanced spectral methods for climatic time series. *Reviews of Geophysics*, 40(1):1003, 2002.
- [7] Nina Golyandina, Vladimir Nekrutkin, and Anatoly A Zhigljavsky. *Analysis of time series structure: SSA and related techniques*. CRC Press, 2010.
- [8] Hossein Hassani. Singular spectrum analysis: methodology and comparison. 2007.
- [9] Hossein Hassani and Anatoly Zhigljavsky. Singular spectrum analysis: methodology and application to economics data. *Journal of Systems Science and Complexity*, 22(3):372–394, 2009.
- [10] William W Hsieh and Aiming Wu. Nonlinear multichannel singular spectrum analysis of the tropical pacific climate variability using a neural network approach. *Journal of Geophysical Research: Oceans (1978–2012)*, 107(C7):13–1, 2002.
- [11] Ian T Jolliffe. *Principal component analysis*, volume 487. Springer-Verlag New York, 1986.
- [12] Bovic Kilundu, Xavier Chiementin, and Pierre Dehombreux. Singular spectrum analysis for bearing defect detection. *Journal of vibration and acoustics*, 133(5), 2011.
- [13] Israel Lopez and Nesrin Sarigul-Klijn. Effects of dimensional reduction techniques on structural damage assessment under uncertainty. *Journal of Vibration and Acoustics*, 133(6):061008, 2011.
- [14] Jonathan Mamou and Ernest J Feleppa. Singular spectrum analysis applied to ultrasonic detection and imaging of brachytherapy seeds. *The Journal of the Acoustical Society of America*, 121:1790, 2007.
- [15] Michael E Mann and Jeffrey Park. Oscillatory spatiotemporal signal detection in climate studies: A multiple-taper spectral domain approach. *Advances in geophysics*, 41:1–131, 1999.
- [16] LE Mujica, J Rodellar, A Fernandez, and A Güemes. Q-statistic and t2-statistic pca-based measures for damage assessment in structures. *Structural Health Monitoring*, 10(5):539–553, 2011.

- [17] LE Mujica, M Ruiz, F Pozo, J Rodellar, and A Güemes. A structural damage detection indicator based on principal component analysis and statistical hypothesis testing. *Smart Materials and Structures*, 23(2):25014–25025, 2014.
- [18] JM Nichols, WA Link, KD Murphy, and CC Olson. A bayesian approach to identifying structural nonlinearity using free-decay response: application to damage detection in composites. *Journal of Sound and Vibration*, 329(15):2995–3007, 2010.
- [19] Seunghee Park, Jong-Jae Lee, Chung-Bang Yun, and Daniel J Inman. Electro-mechanical impedance-based wireless structural health monitoring using pca-data compression and k-means clustering algorithms. *Journal of Intelligent Material Systems and Structures*, 19(4):509–520, 2008.
- [20] David S Stoffer. Detecting common signals in multiple time series using the spectral envelope. *Journal of the American Statistical Association*, 94(448):1341–1356, 1999.
- [21] Irina Trendafilova. An inverse vibration-based approach towards modelling and damage identification in nonlinearly vibrating structures. application for delamination detection in a composite beam. In *Journal of Physics: Conference Series*, volume 382, page 012030. IOP Publishing, 2012.
- [22] Johan A Westerhuis, Theodora Kourti, and John F MacGregor. Comparing alternative approaches for multivariate statistical analysis of batch process data. *Journal of Chemometrics*, 13(3-4):397–413, 1999.
- [23] Keith Worden, Charles R Farrar, Jonathan Haywood, and Michael Todd. A review of nonlinear dynamics applications to structural health monitoring. *Structural Control and Health Monitoring*, 15(4):540–567, 2008.
- [24] A-M Yan, Gaëtan Kerschen, P De Boe, and J-C Golinval. Structural damage diagnosis under varying environmental conditions part ii: local pca for non-linear cases. *Mechanical Systems and Signal Processing*, 19(4):865–880, 2005.
- [25] A-M Yan, Gaëtan Kerschen, Pascal De Boe, and J-C Golinval. Structural damage diagnosis under varying environmental conditions part i: a linear analysis. *Mechanical Systems and Signal Processing*, 19(4):847–864, 2005.
- [26] Y.Zou, L. Tong, and G.P. Steven. Vibration-based model dependent damage (delamination) identification and health monitoring for composite structures-a review. *Journal of Sound and Vibration*, 230(2):357–378, 2000.